Communications on Applied Nonlinear Analysis
ISSN: 1074-133X
Vol 31 No. 6s (2024)

Assessing the Impact of Vaccination Strategies and Re-infection Dynamics on Mycobacterium tuberculosis Transmission by Mathematical Modelling

Naresh Kumar Jothi[1], Lakshmi A.[2], Senthil kumar P[3], Senthil Kumar Dayalan[4a,4b], Ramkumar C.[5]

[1]Associate Professor, Department of Mathematics, Vel Tech Rangarajan Dr. Sagunthala R&D Institute of Science and Technology, Avadi, Chennai, Tamil Nadu, India. Corresponding Author: nareshsastra@yahoo.co.in[1]

[2]Research Scholar, Department of Mathematics, Vel Tech Rangarajan Dr. Sagunthala R&D Institute of Science and Technology, Avadi, Chennai, Tamil Nadu, India.bklakshmimadhesiya81199@gmail.com[2]

[3] Assistant Professor, Department of Mathematics Vel Tech High Tech Dr.Rangarajan Dr.Sakunthala Engineering College, Avadi, Chennai, Tamil Nadu, India,psenthil9159115957@gmail.com[3]

[4a]Research Scholar, Department of Mathematics, Vel Tech Rangarajan Dr. Sagunthala R&D Institute of Science and Technology, Avadi, Chennai, Tamil Nadu, India, senthil.d18@gmail.com [4]

[4b] Assistant Professor, Department of Mathematics, Velammal Institute of Technology, Panchetti, Chennai, Tamil Nadu,

[5]Department Of Mathematics, Bharath Institute of Higher Education and Research, Selaiyur, Chennai, Tamil Nadu, India.scpram@gmail.com[5]

Article History:

Received: *18-05-2024*

Revised: *28-06-2024*

Accepted: *16-07-2024*

Abstract:

In this work, we investigated the consequences of an inadequate vaccination along with other exogenous variables such as treatment-associated re-infection and re-infection among former patients. Our models represent six stages: Susceptible population, Vaccinated population, latently infected population, Rate of induced population, Quarantine population and Rate of recover population. In this model, we find out disease-free equilibrium points, reproduction number R_0 is used to control the re-infection rate in the population. Furthermore, the results suggest that even a subpar Mycobacterium tuberculosis vaccine is always successful at reducing the spread of infectious diseases among the population, even though its general effect improves with greater efficacy and penetration. It is demonstrated that a small percentage of the overall population receives immunization in a stable state and vaccine efficacy plays an equal part in decreasing the burden of disease. Based on the numerical simulation, the establishment of the TB disease is decrease and control by the vaccination coverage and efficacy of the treatment. Using an imperfect vaccine can control mycobacterium in the population. The next-generation matrix approach was utilized to determine the effective reproduction number of the proposed system. The utilization of the exponential theory which provided the disease-free equilibrium is stable and coexists endemic equilibrium point. The Lyapunov function were used to determine the disease is globally asymptotically stable. We find out the non-negative (in variant region). We used random data in MATLAB to figure out the result of the model.

Keywords: Mathematical model, Equilibrium point, Reproduction number, locally asymptotically stable, Non-negative (In variant region), Global stability.

1. Introduction

Mycobacterium tuberculosis (MT), having existed for an extended period has undergone numerous changes in nomenclature. The good news is that the development of mycobacterium begins to take

shape in 1720. The infection caused by a virus might have been inflicted by airborne bacteria that spread to other individuals, as physician Benjamin Marten pointed out in his book A Theory of Consumption. The tuberculosis complex evolved in Africa and developed in the northern part of Africa. Representatives of the tuberculosis complicated (MTBC) which consists of the strains M. tuberculosis, M. africanum, M. bovis (Dassie's bacillus), M. caprae, M. microti, M. mungi, M. orygis and M. pinnipedii have spread the disease to several distinct types of animals. The category may also encompass the M. canettii clade. Despite these reptiles, although variants of MTBC are terribly similar and incorporated in the phylogeny of M. tuberculosis they do not especially merit the status of subspecies; however, for reasons of history, they eventually received that designation. M. proto-tuberculosis is an individual of the distinct species of Mycobacterium that exists in easy-to-colonize colonies, commonly referred to as the M. canettii clade. They produce several distinct species whenever they reproduce, resembling the long-established representatives of the M. tuberculosis organization. All the currently accepted variations of such organisms have been discovered in the Horn of Africa [1-5]. It appears that M. canettii is the primal form of tuberculosis (M. tuberculosis), according to the description from 1969. The tuberculosis bacteria complex's acknowledged members all spread genetically [6-10]. This complex's distinct species relate to multiple state poligo types. Approximately 40,000 and 70,000 years ago, the M. tuberculosis complex's latest common predecessor originated and M. tuberculosis evolved together with human beings. But the findings of a follow-up study that included fragments of 3,000-year-old Peruvian coffins were used for extracting chromosomes from Mycobacterium tuberculosis intricate those who belong and the outcomes showed substantial genomic abnormalities [11-15]. The most contemporary ancestral species of M. tuberculosis intricate was Between 40,000 and 70,000 years old that would suggest a significantly more prevalent predecessor that originated possibly as recently as 6,000 years ago. This would require an embryonic development rate that is significantly lower than the figures derived from heterochromia's samples' genomic analyses. The investigation of over 3000 M. bovis strains from 35 different countries showed that Africa is where this species first originated [16-20].

Two distinct stories are currently being told at the same time about the age of MTBC and how it evolved and spread among humans over time. In one study, the phylogenies of M. tuberculosis and the human genome, which contains mitochondria, showed a great deal of resemblance [21]. The research study states that M. tuberculosis emerged in Africa. Just like individuals do and spread throughout the world by bearing with it contemporary forms of human anatomy. The study determined that the oldest known instance of MTBC developed between 40,000 and 70,000 years ago by comparing this tale with the rate of mutations in M. tuberculosis. Utilizing this chronology, the research revealed that the effective population size of Mycobacterium tuberculosis increased throughout the period of the Neolithic Biological Transition, commencing approximately 10,000 years old. As well as the idea of the tuberculosis strain evolved to adapt to shifting populations of people and that a substantial rise in the overall number of human victims has contributed, at least in part to the pathogen's success in evolution. It was additionally established that the TB lineage that an individual carries is predicted by the geographic region of origin of their human host preceding their transcontinental airline migration [22]. This conclusion might arise from interactions among individuals impacted by common cultural and historical circumstances or from a stable relationship that exists between host populations with tuberculosis generations of organisms [23].

In general, the data provides greater trust for this reasonable assessment of the most recent evolutionary lineages of the MTBC's chronological age. A vertical transfer of genes does not take precedence over DNA propagation because tuberculosis (M. tuberculosis) is a clonal organism. Despite the slow evolution of tuberculosis is recent emergence and spread of bacteria that are resistant to antibiotics in the epidemic pose a rising threat to global health. Antibiotic-resistant tuberculosis (The World Healthcare Organization stated that 3.4% of newly identified cases and 18% of cases had tuberculosis. That had undergone prior chemotherapeutic treatment in 2019. The rate at which tuberculosis that is resistant to drugs develops varies depending on where it occurs. Russia, South Africa, China, and India [24-27].

The hallmark of multidrug-resistant tuberculosis disease (MDR-TB) is an inability to tolerate at least the two first-line medications, rifampin and isoniazid. The significantly modest therapy success rate of 52% is linked to MDR. There is a significant connection between isoniazid and rifampin resistance; in 2019, 78% of TB cases that were reported to be resistant to rifampin also had isoniazid resistance [28-30]. The main cause of rifampin resistance is polymorphisms that confer resistance in the rifampin-resistance predicting region (RRDR) of the rpoB genes. The codons 531, 526, and 516 in RRDR are the ones with the highest prevalence of observed mutations. However, resistance-granting polymorphisms that are more elusive have recently been identified. Isoniazid functionality is achieved by means of the enoyl-acyl transfer protein (ACP)-reductase that depends on NADH, thereby decreasing the process of synthesis of mycolic acid. The gene expressing this is inhA. Therefore, the main cause of isoniazid sensitivity is primarily the consequence of polymorphisms in the glutathione peroxidase gene KatG, or its promoter region, which is essential for isoniazid stimulation and the increasing number of cases of multidrug resistance (MDR) in tuberculosis presents a threat to public health, as demonstrated by the emergence of pre and substantially resistant to medicines (pre-XDR) and XDR-TB strains of the bacterial infection. XDR-TB has been defined by developing resistance to at least another front-line drug, second-line fluoroquinolones, isoniazid and rifampin. As such, the establishment of alternative therapeutic measures is essential. The capability of tuberculosis (M. tuberculosis) to withstand medications is depending on the special cell wall it contains. Mycobacterial organisms are saturated with mycolic acid, a type of long-chain lipid create an extremely strong and not-soluble barrier. Thus, its production is targeted by several antibacterial agents, including isoniazid Still there has been opposition of them. Mycobacterial membrane protein large 3 is an intriguing new pharmacological approach. Transmembrane proteins are composed of proteins that are referred to as mycobacterial protein membrane large (MmpL) complexes are essential to produce the cell wall and the movement of related lipids. MMPL3 is the most crucial of these; its knockout has been demonstrated to be bactericidal. MmpL3 medications exhibit potential as alternate treatment options because of their fundamental features. Throughout the time of resistant antibiotics. Transportation of a substance called Mono mycolate, an essential lipid for cell walls, across the membrane of plasma has been found to be impaired by MmpL3 suppression. Resistant alterations correlate with the transmembrane domain, according to the structure of MmpL3 that was recently reported. Notwithstanding finding evidence of resistance to pre-clinical MmpL3 medications, a low level of environmental resistance was found through examination of the extensive mutational landscape. This suggests that should they become available, MmpL3 inhibitors, which are presently undergoing research studies are likely to

encounter minimal resistance. A glimmer of hope in the struggle against the growing epidemic of tuberculosis is also provided by the fact that many different MmpL3 inhibitors interact well with other antitubercular pharmaceuticals [31-33].

2. Methodology

In this paper, we utilized the non-linear ODE systems of the model S_{TB}-V_{TB}-E_{TB}-I_{TB}-C_{TB}-R_{TB}. N(t) is the total population and they stand for Susceptible population, Vaccinated population, latently infected population, Rate of induced population, Quarantine population and Rate of recover population. Appropriately the recruitment rate of individuals is represented at Λ in the susceptibility compartment framework. For some people, they choose to live a solitary life, because of this, none of these people contracted the illness. Since awareness is thought to be essential for curing the disease, there is also a protective treatment (consciousness) compartment protecting cognizant individuals. Latently exposed people are suffering from a latent tuberculosis infection, meaning they do not actively exhibit the disease; furthermore, those from the susceptibility compartments are γ at a risk of decreasing vaccination-induced infection risk. The pace of vaccination transitions among people ξ who are susceptible. The people's vaccination stage is identified by the rate of transmission variable σ_β, the TB people's progression rate β_u, the vaccine wears off and they are exposed to the disease again at the rate of θ. Is the lack of vaccination inducing a latent increase in the exogenous dissemination rate. TB progression rate and re-infection rate between treated individuals. The individuals who are inside the space are given protective treatment to make certain that the recovered people get transferred to the compartment where they are. A conscious person has also been viewed as an individual who consented to this treatment. The endogenous re-infectionβ_q, the rate of $\beta_p$re-infection from outside and the disease-induced people and Recovery people represented at the rate of π times of TB people is controlled. The rate of τ times of infected TB people is recovered successfully by Quarantine. Since Quarantine and the individuals are completely rebounding from the transmission among those who have been treated. One hundred and ninety-nine out of every 100 TB patients recuperate and are completely healed. In this part, the six distinct groups were created, the next-generation matrix approach was utilized to determine the effective reproduction number of the proposed system. The utilization of the exponential centre theory, which provided $R_0 < 1$ is represented a disease-free equilibrium coexists with a stable endemic equilibrium is stable; we used the Lyapunov function to show that the disease is globally asymptotically stable. Non-negative (in the variant's region) and locally asymptotically stable conditions were implemented. We used MATLAB tool to simulate the spread of diseases among the people.

2.1. Model of the parameters

S_{TB} : Susceptible population

V_{TB} : Vaccinated population

E_{TB} : Latently infected population

I_{TB} : Rate of induced population

C_{TB} : Rate of Quarantine population

R_{TB} : Rate of recover population

Λ : Recruitment rate TB population

γ : Vaccination reduces the risk of infection

θ : The rate of vaccinated population

μ : Natural death rate of the population

ξ : The vaccination rate of people who are susceptible

β_q : Endogenous re-infection population

τ : Disease-induced TB to Quarantine stage

π : Recovery rate of TB

β_u : Progression rate of TB

σ_β : Re-infection among the handled people individually

β_p : Re-infection of the TB people from outside

2.2. Model of the diagram

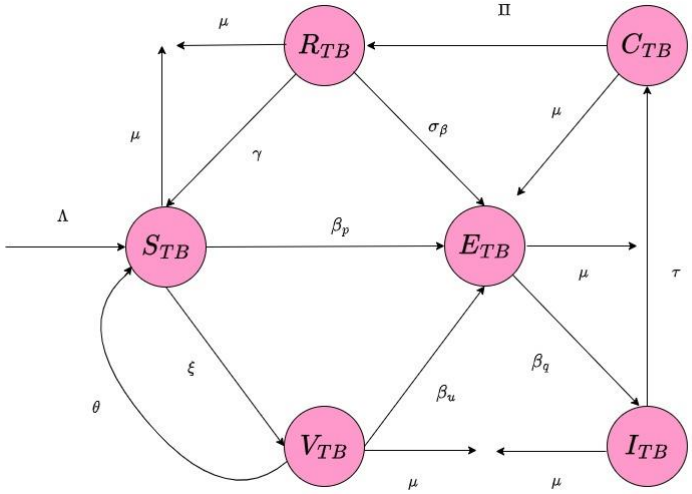

Fig.1 Flowchart of the TB model

2.3. Model of the Equation

$$\frac{dS_{TB}}{dt} = \Lambda + \gamma R_{TB} + \theta V_{TB} - \mu S_{TB} - \xi S_{TB} - \beta_p S_{TB}$$

$$\frac{dV_{TB}}{dt} = \xi S_{TB} - \mu V_{TB} - \beta_u V_{TB} - \theta V_{TB}$$

$$\frac{dE_{TB}}{dt} = \beta_p S_{TB} + \beta_u V_{TB} + \sigma_\beta R_{TB} - \mu E_{TB} - \beta_q E_{TB} \quad (1)$$

$$\frac{dI_{TB}}{dt} = \beta_q E_{TB} - \mu I_{TB} - \tau I_{TB}$$

$$\frac{dC_{TB}}{\mathrm{d}t} = \tau I_{TB} - \mu C_{TB} - \pi C_{TB}$$

$$\frac{dR_{TB}}{\mathrm{d}t} = \pi C_{TB} - \mu R_{TB} - \gamma R_{TB} - \sigma_{\beta} R_{TB}$$

Subject to the non-negative initial conditions specified by

$$S_{TB}(0) > 0\,, V_{TB}(0) > 0\,, E_{TB}(0) > 0\,, I_{TB}(0) > 0\,, C_{TB}(0) > 0\,, R_{TB}(0) > 0$$

It is assumed that for every time $t > 0$, all the parameters in system (1) are positive $t > 0$.

2.4. Disease free equilibrium

$$\frac{dS_{TB}}{\mathrm{d}t} = \Lambda + \gamma R_{TB} + \theta V_{TB} - \mu S_{TB} - \xi S_{TB} - \beta_p S_{TB}$$

Substitute, $V_{TB} = R_{TB} = 0$

$$S_{TB} = \frac{\Lambda}{\mu + \xi + \beta_p}$$

$$\text{DFE} = \left(\frac{\Lambda}{\mu+\xi+\beta_p}, 0, 0, 0, 0, 0\right) \qquad (2)$$

2.5. Endemic equilibrium point

Let $E_* = (S_{TB}^*, V_{TB}^*, E_{TB}^*, I_{TB}^*, C_{TB}^* R_{TB}^*) \in \Omega$ be the equilibrium points of the organization that the equations arrange. First of all, Implementing the condition yields the states of equilibrium.

$$E_* = \{ S_{TB}^* = \frac{\Lambda + \gamma R_{TB} + \theta V_{TB}}{\mu+\xi+\beta_p}, V_{TB}^* = \frac{\xi S}{\mu+\xi+\beta\theta}, E_{TB}^* = \frac{=\beta_p S_{TB} + \beta_u V_{TB} + \sigma_{\beta} R_{TB}}{\mu E_{TB} + \beta_q E_{TB}}, \quad I_{TB}^* = \frac{\beta_q E_{TB}}{\mu I_{TB} + \tau I_{TB}},$$

$$C_{TB}^* = \frac{\tau I_{TB}}{\mu+\pi} \qquad R_{TB}^* = \frac{\pi C_{TB}}{\mu+\gamma+\sigma_{\beta}} \}$$

2.6. Basic Reproduction Number

The next-generation matrix method will be used to determine R_0 after we have distinguished the classes in our model. One of the infectious virus classes is tuberculosis. The TB reproduction number R_0 will therefore be established.

We determine the Reproduction number R_0 and identify the infected cases as I_{TB}.

Let $X = (S_{TB}, V_{TB}, E_{TB}, I_{TB}, C_{TB}, R_{TB})$

F_{TB}be the indication of a rising case of TB

$V_{TB}$is an indication of an outgoing case of TB

$$F_{TB} = \begin{pmatrix} \beta_q \\ 0 \\ 0 \\ 0 \\ 0 \\ 0 \end{pmatrix} V_{TB} = \begin{pmatrix} \mu + \tau \\ \mu + \xi + \beta_p \\ \mu + \beta_u + \theta \\ \mu + \beta_q \\ \mu C_{TB} + \pi C_{TB} \\ \mu + \gamma + \sigma_\beta \end{pmatrix}$$

The derivative of F_{TB} and V_{TB} are given

$$(F_{TB}V_{TB})^{-1} = \frac{\beta_q}{\mu+\tau} \quad (9)$$

$$R_0 = \frac{\beta_q}{\mu+\tau} = R_0 < 1 \quad (10)$$

Reproduction number R_0 is derived from equation (9). Thus, the equilibrium point of the SVEICR model in the disease-free case is asymptotically stable. [table 1].

Theorem 1

(Redundant area) Equation (1)'s set of non-linear differential equations exhibits positive invariance and absorbing in the closed region $\Omega = (S_{TB}, V_{TB}, E_{TB}, I_{TB}, C_{TB}, R_{TB}) \in R_+^6 : 0 \leq N(t) \leq \frac{\Lambda}{\mu}$.

Proof

Differentiating N(t) with respect to time "t"and adding all the right-hand sides of model (1) together gives $N(t) = \Lambda - \mu N$

Based on the non-negativity of model (1) we have that $N(t) = \Lambda - \mu N$

Using Gromwell's inequality, the solution becomes $N(t) \leq \left(\frac{\Lambda}{\mu}\right) + n(0) - \left(\frac{\Lambda}{\mu}\right) e^{-\mu t}$

It follows that $N(t) \leq \left(\frac{\Lambda}{\mu}\right)$ as $t \to \infty$

Hence, $\Omega = \{(S_{TB}, S_{TB}, S_{TB}, S_{TB}, S_{TB}, S_{TB}) \in R_+^6 : 0 \leq N(T) \leq \frac{\Lambda}{\mu}\}$

Thus, in the region of Ω, the hypothesis is well-posed, both in terms of mathematics and biology.

Theorem 2

The proposed model (1) solution set $\{S_{TB}(t), V_{TB}(t), E_{TB}(t), I_{TB}(t), C_{TB}(t), R_{TB}(t)\}$ combined with (2), is positive for all $t > 0$.

Proof

We evaluate equation (1) while taking into consideration the non-linear system of equations.

$$\frac{ds}{dt} = \Lambda + \gamma R_{TB} + \theta V_{TB} - (\mu + \xi + \beta_p) S_{TB}$$

Which means that

$$\frac{ds}{dt} \geq -(\mu + \xi + \beta_p)S_{TB} \quad (11)$$

By integrating, we get

$$S_{TB}(\mathrm{t}) \geq S(0)e^{-(\mu+\xi+\beta_p)t}$$

This goes

$$S_{TB}(t) \geq 0 \quad (12)$$

Theorem 3

Area $\Omega \subset R_+^6$, is defined as follows: the system (1) solutions with initial condition (2) are given.

$$\Omega = \{(S_{TB}(t), V_{TB}(t), E_{TB}(t), I_{TB}(t), C_{TB}(t), R_{TB}(t)) \in R_+^6 \, N(t) \leq \frac{\Lambda}{\mu}\} \quad (13)$$

Proof

By taking the total population, we have

$$\frac{dN(t)}{dt} = \frac{dS_{TB}(t)}{dt} + \frac{dV_{TB}(t)}{dt} + \frac{dE_{TB}(t)}{dt} + \frac{dI_{TB}(t)}{dt} + \frac{dC_{TB}(t)}{dt} + \frac{dR_{TB}(t)}{dt} = \frac{dN}{dt} = \Lambda - \mu N \quad (14)$$

For the entire populace, we have the following:

$$\frac{dN}{dt} = \Lambda - \mu N$$
$$\leq \Lambda - \mu N$$

The equation (14) Solution is presented as

$$N(t) \leq \frac{\Lambda}{\mu N} - \left(\frac{\Lambda}{\mu} - N_0\right) e^{-\mu t} \quad (15)$$

Were $N_0 = N(0)$It is characterized as the population at the start. By using the Brikhoff-Rota theorem, we can

state that if $N_0 < \frac{\Lambda}{\mu}$, then as $t \to \infty$, asymptotically $N(t) \to \frac{\Lambda}{\mu}$ in equation (13) and over the overall population size become $N(t) \to \frac{\Lambda}{\mu}$, then $0 \leq N \leq \frac{\Lambda}{\mu}$.

As a result of this, the A region is where all the model's feasible options converge.

Theorem 4

In the epidemic model, the DFEP Ω is locally asymptotically stable (LAS) if $R_0 < 1$ else unstable.

Proof

Let us now consider the following Jacobian matrix to illustrate the stability requirements at the DFE point denoted by Ω.

Identifying the Jacobi matrix equation (1), which is as follows, is the first stage in the equilibrium point stability evaluation of the SVEICR model for TB infection.

$$J(\Omega) = \begin{vmatrix} -(\mu+\xi+\beta_p) & \theta & 0 & 0 & 0 & \gamma \\ \xi & -(\mu+\beta_u+\theta) & 0 & 0 & 0 & 0 \\ \beta_p & \beta u & -(\mu+\beta_q) & 0 & 0 & \sigma\beta \\ 0 & 0 & \beta_q & -(\mu+\tau) & 0 & 0 \\ 0 & 0 & 0 & \tau & -(\mu+\pi) & 0 \\ 0 & 0 & 0 & 0 & \pi & -(\mu+\gamma+\sigma_\beta) \end{vmatrix} = 0 \qquad (16)$$

Consequently, the characteristic equation (CE) of matrix $J(\Omega)$ can be determined as

$$\Omega(\lambda) = \left(\lambda - \left(\mu+\xi+\beta_p\right)\right)\left(\lambda - (\mu+\beta_u+\theta)\right)\left(\lambda - \left(\mu+\beta_q\right)\right)\left(\lambda - (\mu+\tau)\right)\left(\lambda - (\mu+\pi)\right)(\lambda - \left(\mu+\gamma+\sigma_\beta\right)) = 0 \qquad (17)$$

where

$$\lambda_1 = -(\mu+\xi+\beta p) \qquad (18)$$

$$\lambda_2 = -(\mu+\beta_u+\theta) \qquad (19)$$

$$\lambda_3 = -\left(\mu+\beta_q\right) \qquad (20)$$

$$\lambda_4 = -(\mu+\tau) \qquad (21)$$

$$\lambda_5 = -(\mu+\pi) \qquad (22)$$

$$\lambda_6 = -(\mu+\gamma+\sigma\beta) \qquad (23)$$

consist of the CE's solutions. It is clear that

$\lambda_1, \lambda_2, \lambda_3, \lambda_4, \lambda_5, \lambda_6$ are negative.

Therefore, The DFE is LAS.

2.7 Invariant Region

Theorem 5

Assume that the model solution in the set of equations (1) with initial conditions in $\mathbb{R}_+^6$ is such that it reaches and stays in the set of compact (Ω) as $t \longrightarrow \infty$. A positive invariant set of the model indicates the feasible solution, which is subsequently given by (14).

$$\mathcal{A} = \left\{S_{TB}(t) + V_{TB}(t) + E_{TB}(t) + I_{TB}(t) + C_{TB}(t) + R_{TB}(t) \leq N(t), N(t) \leq \frac{\Lambda}{\mu}\right\}$$

Proof

According to Eq. (14), deviations in N bring about each of the population components to change i.e., ($N = S_{TB} + V_{TB} + E_{TB} + I_{TB} + C_{TB} + R_{TB}$) and we obtain.

$$\frac{dN}{dt} = \Lambda - \mu N \tag{24}$$

considered there was no infection at the primordial stage,

$$\frac{dN}{dt} = \Lambda - N\mu(t) \tag{25}$$

Equation (25) indicates that if $N(t) \geq \frac{\Lambda}{\mu}$, then $\frac{dN(t)}{dt} \leq 0$.

Consequently

$$\frac{dN(t)}{dt} \leq \Lambda - \mu N(t) \tag{26}$$

By rearranging the formula, we obtain

$$\frac{dN(t)}{dt} + \mu N(t) \leq \Lambda \tag{27}$$

which has an integrating factor and is linear: $I.F = e^{\int \mu t} = e^{\mu t}$

The following is how the general solution to (14) can be determined:

$$N(t).(I.F) \leq \int (I.F)dt + k \tag{28}$$

$$N(t).e^{\mu t} \leq \int \Lambda e^{\mu t} dt + k$$

$$N(t).e^{\mu t} \leq \frac{\Lambda e^{\mu t}}{\mu} + k$$

$$N(t) \leq \frac{\Lambda}{\mu} + e^{\mu t}k \tag{29}$$

$N(t = 0) = N_0$ we have

$$N(0) = \frac{\Lambda}{\mu} + k$$

$$\left[N(0) - \frac{\Lambda}{\mu}\right] = k \tag{30}$$

From equation (27) and (28) we have

$$N(t) \leq \frac{\Lambda}{\mu} + (N_0 - \frac{\Lambda}{\mu})e^{-\mu t} \tag{31}$$

As $t \to \infty$ in

The number of individuals decreases to $N(t) \leq$ in (31), as t → ∞. Thus, it follows that at that point, $0 \leq N(t) \leq \frac{\Lambda}{\mu}$, and the directions of the equation of models (1) are constrained in the region $\mathcal{A}$.The proof is now complete. As an illustration, if $\forall t > 0$, the region indicated by,

$$\mathcal{A} = \left\{ \begin{matrix} (S_{TB}(t), V_{TB}(t), E_{TB}(t), I_{TB}(t), C_{TB}(t), R_{TB}(t) \in R^6 \geq 0 \\ S_{TB}(t) + V_{TB} + E_{TB}(t) + I_{TB}(t) + C_{TB}(t) + R_{TB}(t) \leq N(t), N(t) \leq \frac{\Lambda}{\mu} \end{matrix} \right\} \quad (32)$$

symbolizes the model's feasible area Ω must be positively invariant in light of this. Therefore, the model presented in Eqs. (1) is extremely well presented both epidemiologically and analytically. Thus, it is adequate to solely focus on the model's dynamics in the region Ω.

Theorem 6

If $R_0 > 1$, then GAS, which is comprised of area Ω is the endemic's point of equilibrium.

Proof

In order to determine the global stability

Initially, we presume that $R_0 > 1$, meaning that E_* exists. The Lyapunov P function is subsequently obtained and defined as follows:

$$P(Y_1, Y_2 \ldots Y_n) = \sum_i^n \frac{1}{2} [Y_i - Y_i^*]^2 \quad (33)$$

where $Y_i^* =$ The human population equilibrium at the endemic pointE_*.

and $Y_i =$ the population of human classes $(S_{TB}, V_{TB}, E_{TB}, I_{TB}, C_{TB}, R_{TB})$ Based on system (1) equation, accordingly then (32) turns into

$$P((S_{TB}, V_{TB}, E_{TB}, I_{TB}, C_{TB}, R_{TB}) = \frac{1}{2}[(S_{TB} - {S_{TB}}^*) + (V_{TB} - ({V_{TB}}^*) + (E_{TB} - {E_{TB}}^*) + (I_{TB} - {I_{TB}}^*) + (C_{TB} - {C_{TB}}^*) + (R_{TB} - {R_{TB}}^*)]^2 \quad (34)$$

Determine the differential of the mentioned above equation with respect to time t in relation to the following equation (1).

$$\frac{dP}{dt} = [(S_{TB} - {S_{TB}}^*) + (V_{TB} - ({V_{TB}}^*) + (E_{TB} - {E_{TB}}^*) + (I_{TB} - {I_{TB}}^*) + (C_{TB} - {C_{TB}}^*) + (R_{TB} - {R_{TB}}^*)]$$

$$\frac{d}{dt}[S_{TB} + V_{TB} + E_{TB} + I_{TB} + C_{TB} + R_{TB}] \quad (35)$$

Nevertheless, given that from equation (14)

$$\frac{dN(t)}{dt} = [S_{TB} + V_{TB} + E_{TB} + I_{TB} + C_{TB} + R_{TB}] \quad (36)$$

Thus, using equation (24) then (37) results in

$$\frac{dN(t)}{dt} = \Lambda - \mu N \quad (37)$$

$$({S_{TB}}^* + {V_{TB}}^* + {E_{TB}}^* + {I_{TB}}^* + C_{TB} + {R_{TB}}^*) = \frac{\Lambda}{\mu} \quad (38)$$

By substituting the equation (35)-(37) we get (38)

$$\frac{dP}{dt} = \left[N(t) - \frac{\Lambda}{\mu}\right][\Lambda - \mu N(t)]$$

$$\frac{dP}{dt} = \frac{1}{\mu}\,[-\mu N(t) + \Lambda][\Lambda - \mu N(t)]$$

$$\frac{dP}{dt} = \frac{1}{\mu} - [\Lambda - \mu N(t)]^2 \qquad (39)$$

Consequently, Eq. (31), It is clear that $\frac{dP}{dt} < 0$ is a function of Lyapunov strictly speaking, indicating that GAS is the point of a state of equilibrium of endemic E_*. This comprises the components of the area Ω.This implies that the disease tuberculosis (TB) is going to remain prevalent in humans for a significant period of time due to its biological stability.

Once more, in Eq. (31),

$\frac{dP}{dt} = 0 \Leftrightarrow S_{TB} = {S_{TB}}^*, V_{TB} = {V_{TB}}^*, E_{TB} = {E_{TB}}^*, I_{TB} = {I_{TB}}^*, C_{TB} = {C_{TB}}^*, R_{TB} = {R_{TB}}^*$

$\frac{dP}{dt}$ In the region $\mathcal{A}$, positively converge as $t \longrightarrow \infty$.

Thus, this gets close to the proof.

Theorem 7

The mathematical subsystems (1) have unique solutions if it is determined that $\frac{\partial TB_i}{\partial \mathrm{TB}}, TB_i = 1$ are continuous and bounded on D. Let D be the region $\Omega\, TB_i \in R^+$.

Proof

Let equation (1) represented by $TB_1, TB_2, TB_3, TB_4, TB_5$ and TB_6 respectively from equation (1), the following partial derivatives are obtained.

$$\left|\frac{\partial TB_1}{\partial S_{TB}}\right| = \left|\Lambda - \mu S_T - \xi - \beta_p\right| < \infty; \left|\frac{\partial TB_1}{\partial V_{TB}}\right| = |\theta| < \infty \;; \left|\frac{\partial TB_1}{\partial E_{TB}}\right| = 0 < \infty \;;\; \left|\frac{\partial TB_1}{\partial I_{TB}}\right| = 0 < \infty; \left|\frac{\partial TB_1}{\partial C_{TB}}\right| = 0 < \infty; \left|\frac{\partial TB_1}{\partial R_{TB}}\right| = |\gamma| < \infty \qquad (40)$$

The above partial derivatives exist, are continuous and are bounded.

From equation (1), the following partial derivatives are obtained.

$$\left|\frac{\partial TB_2}{\partial V_{TB}}\right| = |\mu - \beta_u - \theta| < \infty \;;\; \left|\frac{\partial TB_2}{\partial S_{TB}}\right| = |\xi| < \infty \;;\; \left|\frac{\partial TB_2}{\partial E_{TB}}\right| = 0 < \infty; \left|\frac{\partial TB_2}{\partial I_{TB}}\right| = 0 < \infty; \left|\frac{\partial TB_2}{\partial C_{TB}}\right| = 0 < \infty; \left|\frac{\partial TB_2}{\partial R_{TB}}\right| = 0 < \infty \qquad (41)$$

Existing, continuous, and constrained are the partial derivatives mentioned above.

From equation (1), the following partial derivatives are obtained.

$$\left|\frac{\partial TB_3}{\partial E_{TB}}\right| = \left|\mu - \beta_q\right| < \infty; \left|\frac{\partial TB_3}{\partial S_{TB}}\right| = \left|\beta_p\right| < \infty; \left|\frac{\partial TB_3}{\partial V_{TB}}\right| = |\beta_u| < \infty; \left|\frac{\partial TB_3}{\partial I_{TB}}\right| = 0 < \infty; \left|\frac{\partial TB_3}{\partial C_{TB}}\right| = 0 < \infty; \left|\frac{\partial TB_3}{\partial R_{TB}}\right| = \left|\sigma_\beta\right| 0 < \infty \qquad (42)$$

Existing, continuous, and constrained are the partial derivatives mentioned above.

From equation (1), the following partial derivatives are obtained.

$\left|\frac{\partial TB_4}{\partial I_{TB}}\right| = |\mu - \tau| < \infty; \left|\frac{\partial TB_4}{\partial S_{TB}}\right| = 0 < \infty; \left|\frac{\partial TB_4}{\partial V_{TB}}\right| = 0 < \infty; \left|\frac{\partial TB_4}{\partial E_{TB}}\right| = |\beta_q| < \infty; \left|\frac{\partial TB_4}{\partial C_{TB}}\right| = 0 < \infty$;
$\left|\frac{\partial TB_4}{\partial R_{TB}}\right| = 0 < \infty$ (43)

Existing, continuous, and constrained are the partial derivatives mentioned above.

From equation (1), the following partial derivatives are obtained.

$\left|\frac{\partial TB_5}{\partial C_{TB}}\right| = |\mu - \pi| < \infty$; $\left|\frac{\partial TB_5}{\partial S_{TB}}\right| = 0 < \infty$;$\left|\frac{\partial TB_5}{\partial V_{TB}}\right| = 0 < \infty$;$\left|\frac{\partial TB_5}{\partial E_{TB}}\right| = 0 < \infty$; $\left|\frac{\partial TB_5}{\partial I_{TB}}\right| = |\tau|0 < \infty$;
$\left|\frac{\partial TB_5}{\partial R_{TB}}\right| = 0 < \infty$ (44)

Existing, continuous, and constrained are the partial derivatives mentioned above.

From equation (1), the following partial derivatives are obtained.

$\left|\frac{\partial TB_6}{\partial R_{TB}}\right| = |\mu - \gamma - \sigma_\beta| < \infty$; $\left|\frac{\partial TB_6}{\partial S_{TB}}\right| = 0 < \infty$;$\left|\frac{\partial TB_6}{\partial V_{TB}}\right| = 0 < \infty$;$\left|\frac{\partial TB_6}{\partial E_{TB}}\right| = 0 < \infty$;$\left|\frac{\partial TB_6}{\partial I_{TB}}\right| = 0 < \infty$;
$\left|\frac{\partial TB_6}{\partial C_{TB}}\right| = |\pi|0 < \infty$ (45)

The above partial derivatives exist, are continuous and are bounded.

Since all the partial derivatives exist and are bounded and defined, the system of equations (1) exists and has solutions.R^6.

3. The predominant equilibrium point's global stability

The Lyapunov functional is utilized to evaluate the global stability of the indigenous equilibrium point Σ_c. To this end, we define the definition that follows

$L(S_{TB}, V_{TB}, E_{TB}, I_{TB}, C_{TB}, R_{TB}) = \frac{1}{2}((S_{TB} - {S_{TB}}^*)+(V_{TB} - {V_{TB}}^*) + (E_{TB} - {E_{TB}}^*) + (I_{TB} - {I_{TB}}^*) + (C_{TB} - {C_{TB}}^*) + (R_{TB} - {R_{TB}}^*))$

The function L has a value greater than zero, and at the predominant equilibrium point Σ_c it equals zero. When we differentiation the function in relation to time, we get

$$\frac{dL}{dt} = (S_{TB} - {S_{TB}}^*)+(V_{TB} - {V_{TB}}^*) + (E_{TB} - {E_{TB}}^*) + (I_{TB} - {I_{TB}}^*) + (C_{TB} - {C_{TB}}^*) + (R_{TB} - {R_{TB}}^*) \quad (46)$$

$$\frac{dS_{TB}}{dt} + \frac{dV_{TB}}{dt} + \frac{dE_{TB}}{dt} + \frac{dI_{TB}}{dt} + \frac{dC_{TB}}{dt} + \frac{dR_{TB}}{dt} = \left(N - \frac{\Lambda}{\mu}\right)(\Lambda - \mu N)$$

$$\leq \left(N - \frac{\Lambda}{\mu}\right)(\Lambda - \mu N) \leq -\left(\frac{\Lambda - \mu N}{N}\right)^2 \leq 0 \quad (47)$$

In cases where, the function is strictly Lyapunov, and from a global asymptotic perspective, the permanent equilibrium point Σ_c is stable. This is valid for $R_o^c > 1$ as this proves that Σ_c exists.

Both epidemiologically and clinically, these results point to an exceptionally long survival period for tuberculosis in humans.

4. Numerical Simulation

The aim of the current research was to examine how the model structure was impacted by vaccination, exogenous re-infection and the rate of transmission. This section primarily presents some of the computational simulation findings in order to demonstrate the mathematical results. Estimating The SVEICR model of mycobacterium tuberculosis transmission has been simulated along with the rate of recruitment of individuals in each compartment, which is the outcome of computing the model with Table 1 displays the models' parameters and initial values.

Parameters	Values	Source
N	50000	Assumption
S_{TB}	8000	Assumption
V_{TB}	7000	Assumption
E_{TB}	9000	Assumption
I_{TB}	10000	Assumption
C_{TB}	9500	Assumption
R_{TB}	6500	Assumption
Λ	0.35	Assumption
γ	0.25	Assumption
θ	0.10	Assumption
μ	0.65	Assumption
ξ	0.75	Assumption
β_q	0.85	Assumption
τ	0.67	Assumption
π	0.6	Assumption
β_u	0.88	Assumption
σ_β	0.95	Assumption
β_p	0.15	Assumption

Table.1

Substituting the disease-free parameter values in Table 1 into Equation (1) we get Equation (48) to Equation (53).

$$\frac{dS_{TB}}{dt} = 0.35 + (0.25)R_{TB} + (0.10)V_{TB} - (0.65)S_{TB} - (0.75)S_{TB} - (0.15)S_{TB} \quad (48)$$

$$\frac{dV_{TB}}{dt} = (0.75)S_{TB} - (0.65)V_{TB} - (0.88)V_{TB} - (0.10)V_{TB} \quad (49)$$

$$\frac{dE_{TB}}{dt} = (0.15)S_{TB} + (0.88)V_{TB} + (0.95)R_{TB} - (0.65)E_{TB} - (0.85)E_{TB} \quad (50)$$

$$\frac{dI_{TB}}{dt} = (0.15)E_{TB} - (0.65)I_{TB} - (0.67)I_{TB} \quad (51)$$

$$\frac{dC_{TB}}{dt} = (0.67)I_{TB} - (0.65)C_{TB} - (0.6)C_{TB} \quad (52)$$

$$\frac{dR_{TB}}{dt} = (0.6)C_{TB} - (0.65)R_{TB} - (0.25)R_{TB} - (0.95)R_{TB} \quad (53)$$

The Tuberculosis free equilibrium point, and its corresponding Eigen values can be found if equation (48-53) is set to zero.

DFE= $(S_{TB}, V_{TB}, E_{TB}, I_{TB}, C_{TB}, R_{TB}) = (\frac{\Lambda}{\mu+\xi+\beta p}, 0, 0, 0, 0, 0)$

$$\lambda_1 = -1.55 \quad (54)$$

$$\lambda_2 = -1.63 \quad (55)$$

$$\lambda_3 = -85.65 \quad (56)$$

$$\lambda_4 = -1.32 \quad (57)$$

$$\lambda_5 = -1.25 \quad (58)$$

$$\lambda_6 = -1.85 \quad (59)$$

If the disease-free parameter values are substituting into Equation (10), the basic reproduction number value is obtained:

$$R_0 = 0.643939 = R_0 < 1. \quad (60)$$

The fundamental reproductive number value is determined through entering the disease-free parameter values into Equations (10), $R_0 = 0.643939 = R_0 < 1$.The results of the simulation for the parameter's values indicate vitality. In this table we are using numerical values and discussed the illusion of individual at stage of TB, we obtained free equilibrium point's T.B. model. We get the result of negative Eigen values and Its control infection of disease among the populations and final stage is stable. The fundamental reproductive number value is determined through entering the disease-free parameter values and the reproduction rate $R_0 < 1$.

5. Discussion

Here we discussed the simulation of the SVEICR model of tuberculosis transmission of six compartment stage. S_{TB}-V_{TB}-E_{TB}-I_{TB}-C_{TB}-R_{TB}. In this part we used random data, to apply some mathematical loop to control the infection of the TB disease in the individual population. We showed some result and diagram of the SVEICR model in the below discussion part. For ease, we used some random data to find out the infected cases in numerical simulation. Susceptible S_{TB} individuals move to the vaccinated stage V_{TB}, the latently exposed stageE_{TB},the infected stage of peopleI_{TB} , the Quarantine stage of C_{TB} people and the recovered stage of R_{TB}, all the stages of infected people are controlled and stable. We analysed the endemic equilibrium point's stability in this SVEICR model. We used MATLAB to explore the results of the diseases are controlled and stable.

In fig.2 the evaluation of SVEICR model we used, some random variables and parameters are measured and to find out the total population of infected people in the TB region. $\Lambda =$ 27.2; $\gamma = 0.3$; θ =0.4; μ =0.2; ξ =0.3; β_p =0.5; β_q =0.6; β_u =0.54; σ_β =0.2; τ =0.3; $\pi = 0.7$.

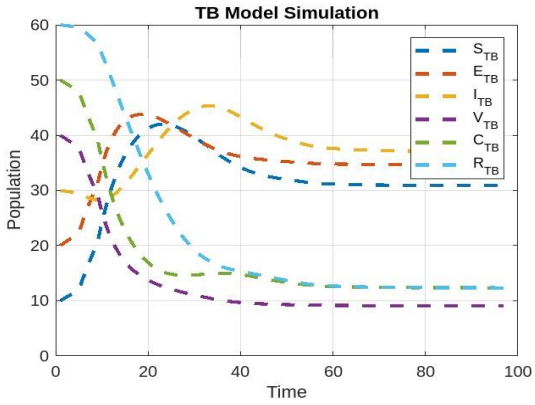

Fig.2 Stability analysis of total TB population $\Lambda = 27.2$.

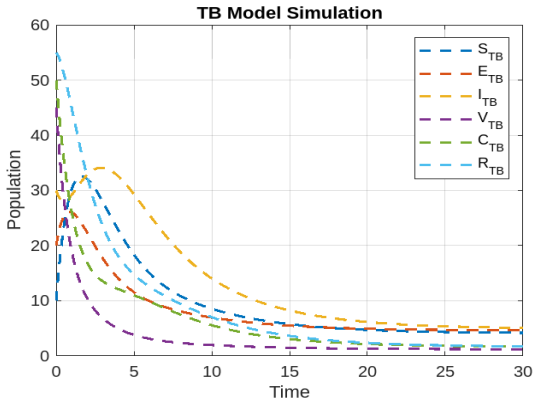

Fig.3 Stability analysis of total TB population $\Lambda = 3.62$.

In fig.3 we used some random data to find out the total population of infected people in TB. All the stages of the people are controlled and stable.

$\Lambda = 3.62$; $\gamma = 0.3$; $\theta = 0.4$; $\mu = 0.2$; $\xi = 0.3$ $\beta_p = 0.5$; $\beta_q = 0.6$; $\beta_u = 0.54$; $\sigma_\beta = 0.2$; $\tau = 0.3$; $\pi = 0.7$.

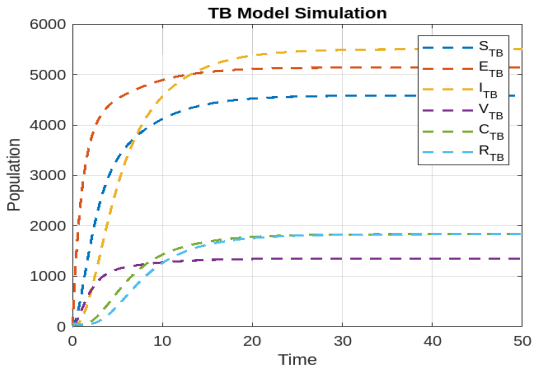

Fig.4 Stability analysis of TB population $\Lambda = 4051.5419$.

In fig.4 we used some random data to find out the infection of TB peoples and short out infected region, all the four stages are controlled and stable. $\Lambda = 4051.5419$; $\gamma = 0.3$; $\theta = 0.4$; $\mu = 0.2$; $\xi = 0.3$; $\beta_p = 0.5$; $\beta_q = 0.6$; $\beta_u = 0.54$; $\sigma_\beta = 0.2$; $\tau = 0.3$; $\pi = 0.7$

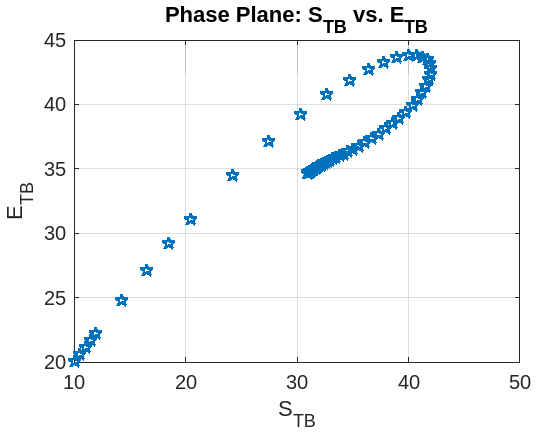

Fig.5 Population trends unveiled: A time-based analysis $\Lambda = 27.2$.

In fig.5 we used some random data to find out the infection of TB peoples and short out infected region, we compared the susceptible and exposed stage of infected people in time-based analysis; both stages are controlled and stable.Λ =27.2; $\gamma = 0.3$; θ =0.4; μ =0.2; ξ =0.3; β_p =0.5; β_q =0.6; β_u =0.54 ; $\sigma_\beta = 0.2$; τ=0.3; π =0.7.

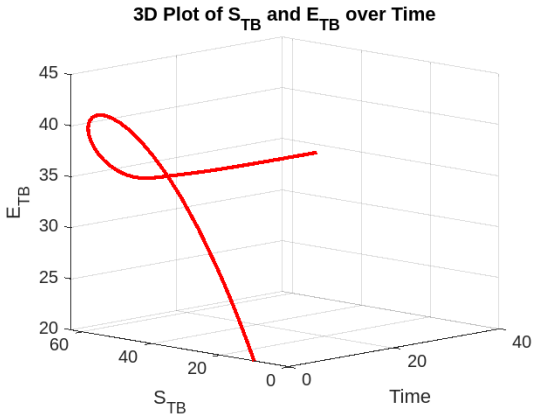

Fig.6 3D Trajectory of susceptible and exposed stage of TB population.

In fig.6 we demonstrate the simulation of 3D trajectory in dynamic perspectives. We used random data to find out the infection, the susceptible and exposed stage of TB population are controlled and stable.

Λ = 27.2; $\gamma = 0.25$; θ =0.35; $\mu = 0.15$; ξ =0.25; $\beta_p = 0.6$; $\beta_q = 0.4$; $\beta_u = 0.45$; $\sigma_\beta =$ 0.3; τ =0.25; $\pi = 0.6$.

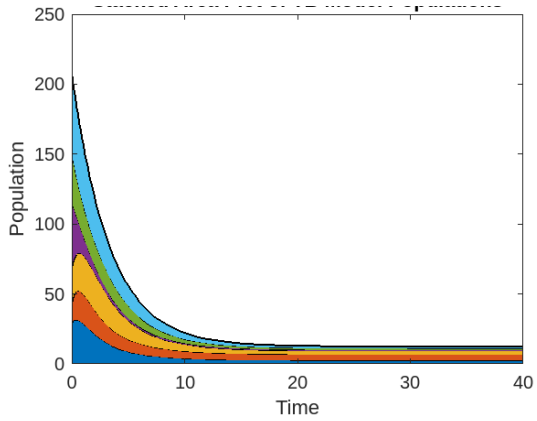

Fig.7.1 Stacked area plot of TB model population.

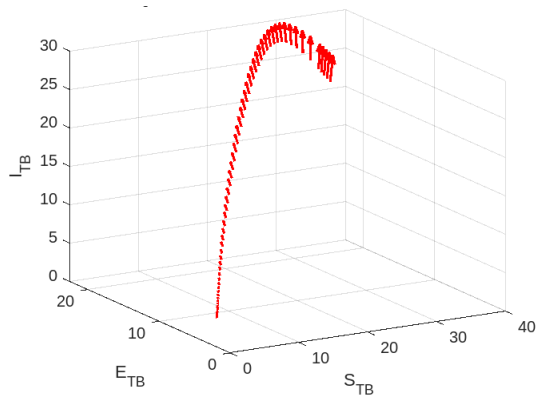

7.2 Quiver plot of TB model vector field.

In fig.7.1 we examined the all the stages of TB population in incidence graph, we stacked area plot of TB.

fig.7.2- Quiver plot of TB model vector field , the infected,exposed and suscceptible stages of TB people are controlled.In both figuer we used random data to find out the infection among the people.

Λ =3.6; $\gamma = 0.2$; θ =0.5; μ =0.3; ξ =0.25; β_p =0.6; β_q =0.7; β_u =0.6; $\sigma_\beta = 0.1$; τ =0.4; π = 0.55.

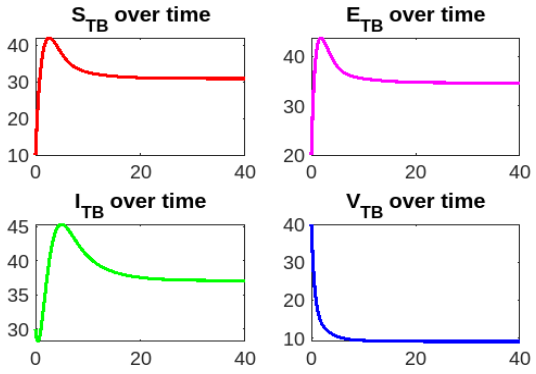

Fig.8 Population of dynamics of TB model.

In fig.8.Illustrates the effects of different reduction in susceptibility to the disease by vaccinated, infected, as well as exposed individuals at the population dynamics of TB patients that are stable and controlled through the use of data collected at random. Λ =27.2; γ = 0.3; θ =0.4; μ =0.2; ξ =0.3; β_p =0.5; β_q =0.6; β_u =0.54; σ_β =0.2; τ =0.3; π = 0.7.

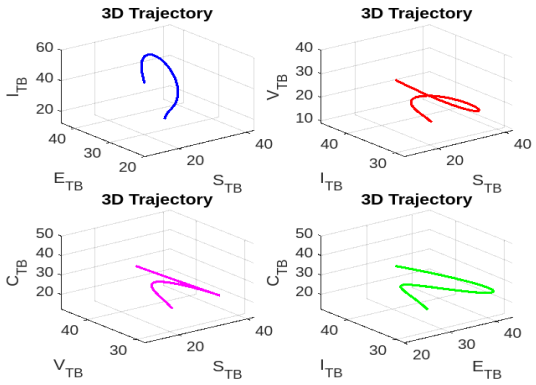

Fig.9 Visualising the dynamics: Differential equation solution.

In fig.9.We show that the predominant equilibrium point is asymptotically stable locally with respect to global stability. As can be observed from the diagram, we deployed an analytical loop to control the infection in the tuberculosis population by analysing the trajectory of the solutions of the system model (1).Λ =27.2; γ =0.3; θ =0.4 ; μ =0.2 ; ξ =0.3; β_p =0.5 ; β_q =0.6 ; β_u =0.54 ; σ_β =0..2; τ =0.3; π = 0.7.

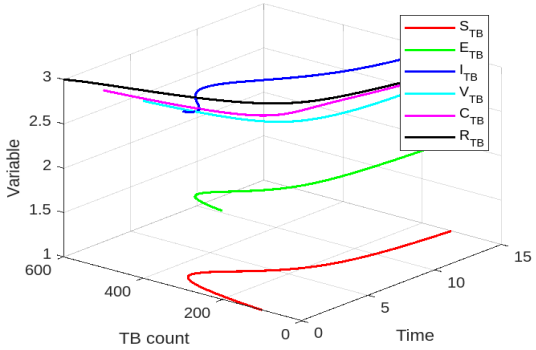

Fig.10 TB variation over time in all stages.

In fig.10 we used random data to find out the infection of TB in the infected region of people.in this figure each stage of TB is varies from one stage to another stage, all the stages are controlled and stable.

Λ =1.32; $\gamma = 0.3$; θ =0.4; $\mu = 0.2$; ξ =0.3; $\beta_p = 0.5$; β_q =0.6; β_u =0.54; σ_β =0.2; τ =0.3; $\pi = 0.7$.

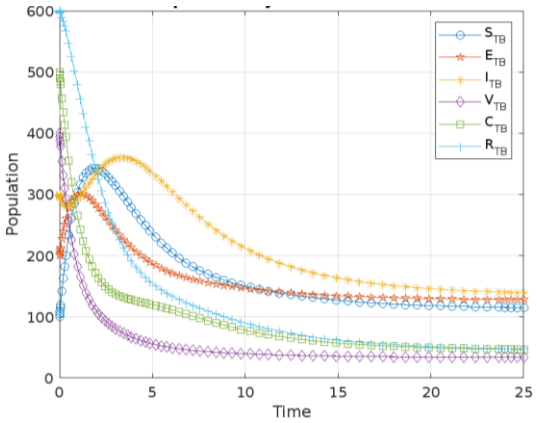

Fig.11.The stability of the rate of population Dynamic over time Λ =1.34.

In fig.11. The structure of the model (1) variation as a function of time (years) is displayed The TB-free equilibrium's neighbourhood stability is shown in this figure. The figure demonstrates how the progressions of the system model (1)'s solution approximate to the point of equilibrium that is free of disease. In accordance with this figure, it can be demonstrated that the disease-free state is GAS if $R_O < 1$, as the disease cannot propagate throughout the entire population if $R_O < 1$. Λ =1.34; γ = 0.3; θ =0.4; μ = 0.2; ξ =0.3; β_p =0.5; β_q =0.6; β_u =0.54; σ_β =0.2; τ =0.3; π =0.7.

6. Conclusion

In this work, we generated a predictable computational model to acquire an elementary comprehension of the changing behaviour of SVEICR model, we explored the impact of limited vaccination and other external factors on the dynamics of tuberculosis disease transmission. The population at risk of tuberculosis has been divided into six distinct groups. We determined the actual reproduction number R_0. The next-generation matrix approach was utilized. In instances where a specific epidemiological threshold quantity known as the effective reproduction number $R_0 < 1$ its falls below unity. TB dynamics were represented by six distinct compartments that possessed a locally asymptotically secure disease-free equilibrium. The disease may continue to spread throughout the population even if the $R_0 < 1$ the basic epidemiological requirement is met; nevertheless, appropriate TB spread control in a population was still required. The condition was fully defined by the initial size of the population (see Figure 4). In addition, the contrast of both high and low vaccination of population dynamics coverage rates was investigated (refer to Figure 8). In comparison to the high case, it was discovered that the lower case had a higher endemic equilibrium. Non-negative (in the variant's region) and locally asymptotically stable conditions were implemented. The utilizing global stability, it can be figured out that the intrinsic equilibrium point

$\Sigma_c$is asymptotically stable worldwide since both the existence of Σ_c and $\frac{dL}{dt} < 0$ suggest the equation is rigorously Lyapunov. This result suggests that epidemically disseminated tuberculosis (TB) will persist in the population of humans for a considerable period when used in a non-linear susceptibility stage. In accordance with the SVEICR simulation under investigation, the use of an inadequate vaccine may occasionally result in adverse consequences for the general population. Nevertheless, it has been determined that an inadequate vaccine continues to reduce the burden of disease and have a positive epidemiological impact on people in general, even if its overall impact is enhanced by increased vaccine efficacy and protection rate. We used MATLAB software to simulate the results of the TB infection in the people.

Institutional Review Board Statement:Not applicable.

Informed Consent Statement: Not applicable.

Data Availability Statement: The data used to support the findings of this study are included within the article.

Conflicts of Interest: The writers declare that no conflicts of interest exist.

Reference

[1] Nyerere, N. Modeling the Effect of Screening and Treatment on the Transmission of Tuberculosis Infections, Mathematical Theory and Modeling. 4, 7, 2014.

[2] Richardson, M. et al Multiple Mycobacterium tuberculosis strains in early cultures from patients in a high incidence community setting, Journal of Clinical microbiology. 40, 2750–2754, 2002.

[3] Yang, HM. Raimundo, SM. Assessing the effects of multiple infections and long latency in the dynamics of tuberculosis, Theoretical biology and medical modeling. 7, 41, 2010.

[4] Behr, MA. Tuberculosis due to multiple strains: a concern for the patient? A concern for tuberculosis control? American journal of Respiratory and critical care medicine. 169, 554–555, 2004.

[5] Bisuta, S.F. Kayembe, P.K., Kabedi, M.-J.B., Situakibanza, H.N., Ditekemena, J.D., Bakebe, A.M., Lay, G.O., Mesia, G.K., Kayembe, J.-M.N., Fueza, S.B.: Trends of bacteriologically confirmed pulmonary tuberculosis and treatment outcomes in Democratic Republic of the Congo: 2007–2017, Annals of African medicine. 11, 2974–2985 2018.

[6] Feng, Z.Castillo Chavez, C. Capurro, AF. A model for tuberculosis with exogenous re-infection, Theoretical Population Biology.57, 235–247, 2000.

[7] Bowong, S. Emvudu, Y. Moualeu, DP. Tewa, JJ. Mathematical properties of a Tuberculosis model with two differential infectivity and N latent classes, Journal of Nonlinear Science and Applications.13–26, 2010.

[8] Naresh, R. Pandey, S. Shukla, JB. Modeling the cumulative effect of ecological factors in the habitat on the spread of Tuberculosis, International Journal of Biomathematics. 2, 339–355, 2009.

[9] Magombedze, G. Garira, W. Mwenje E Mathematical modeling of chemotherapy of human TB infection, Journal of Biological systems.14, 509–553, 2006.

[10] Humphreys, H. Control and prevention of health care associated tuberculosis: the role of respiratory isolation and personal respiratory protection, Journal of Hospital infection. 66, 1–5, 2007.

[11] Colditz, G.A.; Brewer, T.F.; Berkey, C.S.; Wilson, M.E.; Burdick, E.; Fineberg, H.V.; Mosteller, F. Efficacy of BCG vaccine in the prevention of tuberculosis: meta-analysis of the published literature. JAMA, 271, 698–702, 1994.

[12] Nguipdop-Djomo, P. Heldal, E.; Rodrigues, L.C.; Abubakar, I.; Mangtani, P. Duration of BCG protection against tuberculosis and change in effectiveness with time since vaccination in Norway: A retrospective population-based cohort study, Lancet Infectious Diseases. 16, 219–226, 2016.

[13] Gomes, M.G.M.; Franco, A.O.; Gomes, M.C.; Medley, G.F. The re-infection threshold promotes variability in tuberculosis epidemiology and vaccine efficacy. Proc. R. Soc. Lond. Ser, B Journal of Biological Science. 271, 617–623, 2004.

[14] Porco, T.C.; Blower, S.M. Quantifying the intrinsic transmission dynamics of tuberculosis, Theoretical Population Biology. 54, 117–132,1998.

[15] Adewale, S. O., Podder, C. N., Gumel, A. B. Mathematical analysis of a TB transmission model with DOTS. Can, Applied Mathematics. 17, 1–36,2009.

[16] Egonmwan, A.O.; Okuonghae, D. Analysis of a mathematical model for tuberculosis with diagnosis, Journal of computational and Applied Mathematics. 59, 129–162, 2009.

[17] Ullah, S.; Khan, M.A.; Farooq, M.; Gul, T. Modeling and analysis of Tuberculosis (TB) in Khyber Pakhtunkhwa, Pakistan, Mathematics, and computers simulation. 165, 181–199, 2019.

[18] Bloom, B.R.; Murray, C.J. Tuberculosis: Commentary on a reemergent killer, Science. 257, 1055–1064, 1992.

[19] Behr, M.A. Tuberculosis Due to Multiple Strains: A Concern for the Patient? A Concern for Tuberculosis Control? Annals of the American Thoracic Society.169, 554–555, 2004.

[20] Dolin, P.J. Raviglione, M.C. Kochi, A. Global tuberculosis incidence and mortality during 1990–2000. Bull, World health Organiztion.72, 213,1994.

[21] Castillo-Chavez, C. Song, B. Dynamical models of tuberculosis and their applications, Mathematical Biosciences and Engineering.1, 361, 2004.

[22] Richardson, M. Carroll, N.M. Engelke, E. van der Spuy, G.D.; Salker, F. Munch, Z. van Helden, P.D. Multiple Mycobacterium tuberculosis strains in early cultures from patients in a high-incidence community setting, Journal of Clinical Microbiology.40, 2750–2754, 2002.

[23] Naresh Kumar Jothi, Lakshmi. A, Development and Analysis of Malaria Vector by Mathematical Modeling; Lecture Notes in Electrical Engineering: Springer. 1116, 551-562, 2024.

[24] Blower, S.M. Mclean, A.R. Porco, T.C. Small, P.M. Hopewell, P.C. Sanchez, M.A. Moss, A.R. The intrinsic transmission dynamics of tuberculosis epidemics, Nature Medicine. 1, 815–821,1995.

[25] Brogger, S. Systems analysis in tuberculosis control, A model American review of respiratory diseases. 95, 419–434, 1967.

[26] Naresh Kumar Jothi,Vadivelu, V. Senthil Kumar Dayalan, Jayant Giri, Wesam Atef Hatamleh, and Hitesh Panchal, Dynamic interactions of HSV-2 and HIV/AIDS: A mathematical modeling approach, AIP Advances. 14, 1-16, 2024.

[27] Zargar. F.A and Khanday. M.A, Mathematical analysis on the dynamics of COVID-19 in India using SIR Epidemic Model, Mapana Journal of Sciences. 19, 3, 2020.

[28] Castillo-Chavez, C. and Feng, Z. to treat or not to treat: The case of tuberculosis, Journal of Mathematical Biology. 35, 629–656,1997.

[29] Naresh Kumar Jothi, M. L. Suresh, and T. N. M. Malini Mai, “Mathematical model for the control of life cycle of feminine Anopheles mosquitoes,” Int. J. Recent Technol. Eng.8(3), 5316–5319 2019.

[30] Naresh Kumar Jothi, Anusha Muruganandham, T. Vivekanandan, T. Stalin, and Senthil Kumar Dayalan, Mathematical analysis of control strategies and stability in feminine Aedes aegypti, J. Asiat. Soc. Mumbai 96, 115–125 2023

[31] T. A. Kenyon, S. E. Valway, W. W. Ihle, I M Onorato, Castro, Transmission of multidrug-resistant Mycobacterium tuberculosis during a long airplane flight, New England Journal of Medicine. 334, 933–938,1996.

[32] Kar, T.K.; Mondal, P.K. Global dynamics of a tuberculosis epidemic model and the influence of backward bifurcation, Journal of Mathematical Biology. Algorithms. 11, 433–459, 2012.

[33] Naresh Kumar Jothi, Anusha Muruganandham, T. Stalin, T. and Senthil Kumar Dayalan, Ecological dynamics and control strategies of the feminine anopheles Stephensi using Volterra–Lyapunov function, J. Oriental Inst. 72, 117–127, 2023.